Ann. Geophys., 31, 135–144, 2013
www.ann-geophys.net/31/135/2013/
doi:10.5194/angeo-31-135-2013

Annales Geophysicae

Multi-instrument comparisons of D-region plasma measurements

M. Friedrich[1], **K. M. Torkar**[2], **U.-P. Hoppe**[3,4], **T.-A. Bekkeng**[4], **A. Barjatya**[5], **and M. Rapp**[6,*]

[1]Graz University of Technology, Graz, Austria
[2]Space Research Institute, Austrian Academy of Sciences, Graz, Austria
[3]Norwegian Defence Research Establishment, Kjeller, Norway
[4]University of Oslo, Oslo, Norway
[5]Embry-Riddle Aeronautical University, Daytona Beach, FL, USA
[6]Institute for Atmospheric Physics, Kühlungsborn, Germany
[*]now at: German Aerospace Center, Institute of Atmospheric Physics, Oberpfaffenhofen, Germany

Correspondence to: M. Friedrich (martin.friedrich@tugraz.at)

Received: 31 August 2012 – Revised: 19 November 2012 – Accepted: 3 January 2013 – Published: 29 January 2013

Abstract. The ECOMA (Existence and Charge state Of Meteoric dust grains in the middle Atmosphere) series of sounding rocket flights consisted of nine flights with almost identical payload design and flight characteristics. All flights carried a radio wave propagation experiment together with a variety of plasma probes. Three of these measured electron densities, two ion densities. The rockets were all launched from the Andøya Rocket Range, Norway, in four campaigns between 2006 and 2010. Emphasis is on the final three flights from 2010 where the payloads were equipped with four instruments capable of measuring plasma densities in situ, among them a novel probe flown for the first time in conjunction with a wave propagation experiment. Deviation factors of all probe data relative to the wave propagation results were derived and revealed that none of the probe data were close to the wave propagation results at all heights, but – more importantly – the instruments showed very different behaviour at different altitudes. The novel multi-needle Langmuir probe exhibits the best correlation to the wave propagation data, as there is minimal influence of the payload potential, but it is still subject to aerodynamics, especially at its location at the rear of the payload. For all other probe types, the deviation factor comes closer to unity with increasing plasma density. No systematic difference of the empirical deviation factor between day and night can be found. The large negative payload potential in the last three flights may be the cause for discrepancies between electron and ion probe data below 85 km.

Keywords. Ionosphere (Auroral ionosphere)

1 Introduction

The series of nine sounding rockets of the ECOMA project was dedicated to the investigation of large charged or neutral particles in the mesosphere. In summer the largest of these particles are ice crystals, but during all seasons aerosols and cluster ions are expected to be present. Table 1 summarises the launch times and dates, and the most relevant geophysical conditions of the ECOMA flights. The primary instrument contained on each payload was the ECOMA particle detector flown on all flights, but the other instrumentation varied somewhat in the four campaigns. No results are reported for the first two flights because the probes' performance was affected by another instrument within the payload. The flights ECOMA-3 to -6 included two instruments providing data on ion density and two instruments measuring electron density; however, the data from those flights are not presented here in detail, but only listed summarily for completeness. The first campaign with three flights was conducted in the noctilucent cloud (NLC) season when ice crystals were expected, another one with two flights was conducted during background conditions (outside the NLC season), and the final campaign was dedicated to the investigation of mesospheric effects of a meteor shower. The data from these latter three flights (ECOMA-7 to -9) are presented here in detail.

The final campaign conducted in December 2010 (ECOMA-7, -8 and -9) carried an additional novel probe to measure electron densities with high resolution. Since the payloads and the trajectories were almost identical, these latter three flights provide a rare opportunity to assess the

Table 1. List of rockets and the geophysical conditions prevailing at the flights of the present analysis; emphasis is on flights 7 to 9.

Code	Date	Time, UT	Zenith angle, deg	Solar flux, sfu	Sunspot number	Conditions
ECOMA-3	3 Aug 2007	23:22	93.2	70.4	7	NLC
ECOMA-4	30 Jun 2008	13:22	50.9	66.7	0	NLC
ECOMA-5	7 Jul 2008	21:24	86.5	65.5	0	NLC, sporadic *E*
ECOMA-6	12 Jul 2008	10:46	47.7	64.9	0	NLC
ECOMA-7	4 Dec 2010	04:21	112.9	87.4	31	before meteor shower
ECOMA-8	13 Dec 2010	03:24	119.1	87.7	28	peak of meteor shower
ECOMA-9	19 Dec 2010	02:36	123.6	80.9	0	after meteor shower

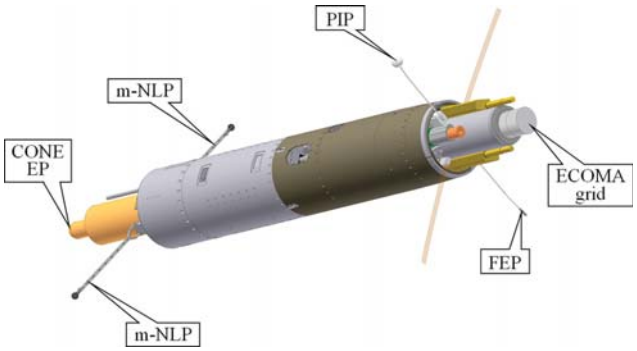

Fig. 1. ECOMA payload in-flight configuration after payload separation at 70 s. PIP: positive ion probe; FEP: forward electron probe (fixed-bias Langmuir probe); m-NLP: multi-needle Langmuir probe; CONE EP: electron probe as part of the CONE instrument (on upleg in the wake).

strengths and weaknesses of the various instruments under different geophysical conditions. The instrument CONE (COmbined sensor for Neutrals and Electrons) is a combination of an ionization gauge and a fixed-bias Langmuir probe. Since it was mounted at the rear of the payload, whereas all other instruments are located near the front, its data are difficult to compare with the others due to opposite ram/wake effects. The CONE data are most useful on downleg, whereas the other instruments function best on upleg. Therefore, we concentrate on the upleg of the flights and leave the CONE results out of this report of the investigations.

2 Instrumentation

2.1 Wave propagation experiment

When a magnetic field is superimposed on a plasma, an electromagnetic wave propagates in ordinary and extraordinary modes (o, x). The ionosphere and the Earth's magnetic field represents such a scenario. The accepted theory of radio wave propagation in a magneto-plasma is described by Sen and Wyller (1960), and a somewhat more generalised form is given by Friedrich et al. (1991). Both refractive indices are complex, i.e. their real parts control the phase velocity, the imaginary parts lead to absorption. The refractive indices are functions of the electron density, N_e, the wave frequency, the strength and direction of the magnetic field and the collision frequency. In the height region where the collision frequency matters ($<$100 km), it is proportional to the atmosphere's pressure (Thrane and Piggott, 1966). In a study using collision frequencies obtained from many sounding rocket flights, Friedrich and Torkar (1983) derived a proportionality factor to pressure of $6.41 \times 10^5\,\mathrm{m^2\,s^{-1}\,N^{-1}}$, which agrees with the laboratory value of Phelps and Pack (1959) within the accuracy of the derivation.

When the magnetic field has a component in propagation direction, the polarisation orientation of a linearly polarised wave rotates (Faraday rotation). The rotation of the plane of the polarisation relative to that of the antenna on the ground provides a measure of the electron content (electrons $\mathrm{m^{-2}}$) between ground and rocket; differentiation with respect to altitude yields electron density N_e (electrons $\mathrm{m^{-3}}$). The easiest way to make use of this phenomenon is to rotate an antenna with the spinning rocket and observe the modulation pattern (double-spin modulated). A signal maximum is observed when the local polarisation is parallel to the receiving antenna, and a minimum occurs when it is at 90°. By using a spatial reference such as a magnetometer, a gyro or a Sun sensor, one can establish the Faraday rotation as a function of altitude. Most rocket payloads, notably after separation from the motor (second stage), not only rotate with the intended, pre-determined spin (3 to 5 Hz), but will generally also exhibit coning with periods of a few seconds and opening angles of up to, say, 20°. Unfortunately, the coning motion modulates the spatial reference resulting in an apparent Faraday rotation superimposed on the one due to the electron content. Since the receivers are fed in series from the same antenna, one can eliminate the influence of coning by deriving the phase between the receiver outputs of different frequencies (differential Faraday rotation). Except if only one frequency is available – i.e. when the lower ones are all absorbed or reflected – we use an aspect sensor as the spatial reference.

2.2 Fixed-bias Langmuir probe

According to the basic derivation by Smith (1969), the electron current density, i, to a cylindrical probe that is biased with a voltage, V, is

$$i = i_0\sqrt{1+\frac{eV}{kT}}, \quad (1)$$

where $i_0 = \frac{N_e e v_{th}}{4}$ is the current density to a stationary probe, and $v_{th} = \sqrt{\frac{8kT}{\pi m_e}}$ is the thermal velocity of the electrons. For $eV/kT >> 1$, the current, I, collected by a cylindrical probe with length, l, and diameter, d, becomes independent of temperature:

$$I = N_e l d\sqrt{\frac{e^3 V\pi}{2m_e}}. \quad (2)$$

A cylindrical probe is thus largely unaffected by the electron temperature, and by putting it on a boom long enough to always reach outside the shock cone, it should – at least within the flow conditions on upleg – ideally not experience any spin modulation of the measured signal on the FEP (forward electron probe; see Fig. 1). The actual probe of the final ECOMA flights (-7, -8 and -9) was 14 mm long, had a diameter of 3 mm, and was at a bias potential of +2.5 V. The length of the boom was 500 mm from the payload.

2.3 Spherical ion probe

A gridded sphere (45 mm diam, ca. 90 % transparency) with a negatively biased inner collector measures a current by (a) the thermal motion of the ions, and (b) the motion of the probe through a stationary plasma. Typical thermal velocities of ionospheric ions are on the order of 300 to 600 m s^{-1}, hence usually lower than the velocity of the probe (the rocket) passing through the plasma. Once the rocket velocity exceeds the ion velocity by a factor of two or more, the current measured by such a device is largely proportional to the probe's collection cross section, the grid's transparency and the rocket velocity (Folkestad, 1970). An accurate knowledge of the ions' thermal velocity (their mass and temperature) is therefore not crucially important in view of the much larger velocity of the rocket. This probe is also mounted in the forward section on a long boom (opposite FEP) to always reach outside the shock cone (PIP: positive ion probe; Fig. 1).

2.4 Multi-needle Langmuir probe

In addition to the above described probes, the final three ECOMA flights carried a novel instrument, namely a multi-needle Langmuir probe (m-NLP). This instrument was flown earlier on two rocket payloads, but the present flights for the first time provide opportunities to test the absolute values by comparison to the wave propagation data. According to Eq. (2), the current drawn by a thin, fixed-bias Langmuir probe is proportional to $\sqrt{V}$, where V is the voltage applied to the probe relative to an a priori unknown payload potential. As long as V is larger than the floating potential of the payload, the squares of the currents of probes with different voltages will be linearly related to the applied voltage. This idea, developed at the University of Oslo, was tested in a plasma chamber (Bekkeng et al., 2010) and flown for the first time on a sounding rocket using four very thin probes ("needles"; Jacobsen et al., 2010). On the rockets ECOMA-7, -8 and -9, the four needles, much thinner than the fixed-bias probe described above (0.5 by 25 mm), were on two booms 400 mm from the payload, opposite to each other at the rear of the payload (Fig. 1). Due to this unfavourable location only one boom (with two needles) at a time was in the ram and thus measured the presumed "good" current values of the undisturbed plasma, whereas the other in general was in the wake and thus recorded a current less likely representing the ionospheric electron density. Since we want to test the credibility of the measurements by checking if the currents of all needles with the different biases indeed obey the $\sqrt{V}$ law, we need the "good" values of all four needles at the same time; this is achieved by interpolating between consecutive "good" (ram) values (one per spin period) and forming the $\sqrt{V}$ relation at any desired time increment. The intersect of the extrapolation of the currents from the different needles to zero current yields the payload potential (see the paper dedicated to this aspect by Bekkeng et al., 2013). The measurements of this probe begin later than those of the other plasma instruments because the relevant booms at the rear section could only be deployed after payload separation, i.e. at about 83 km on upleg.

In the present three ECOMA flights, the probe biased at +4.29 V deviates from the straight line of I^2 vs. V given by the three remaining probes. Probes biased with about the same potential on the Investigation of Cusp Irregularities 3 (ICI-3) payload from Spitsbergen and on the 36.273 MICA payload flown from Poker Flat, Alaska, show the same behaviour. By comparing to probe characterisation experiments carried out in the plasma chamber at ESTEC, this deviation is believed to be caused by a difference in work function between the bootstrap part of the miniaturised Langmuir probe and the collecting element of the probe. Final conclusions concerning this behaviour will only be available when more is learned about the probe characteristics during future testing at ESTEC. The quality of the I^2 vs. V fit reaches values of between 0.97 and 0.99 above typically a 90 km altitude; this does not translate into electron density error bars, but indicates that the optimum performance of the instrument has been reached.

2.5 ECOMA shielding grid

The entrance of the particle detector ECOMA is shielded from the ambient plasma by two grids biased by ±3 V,

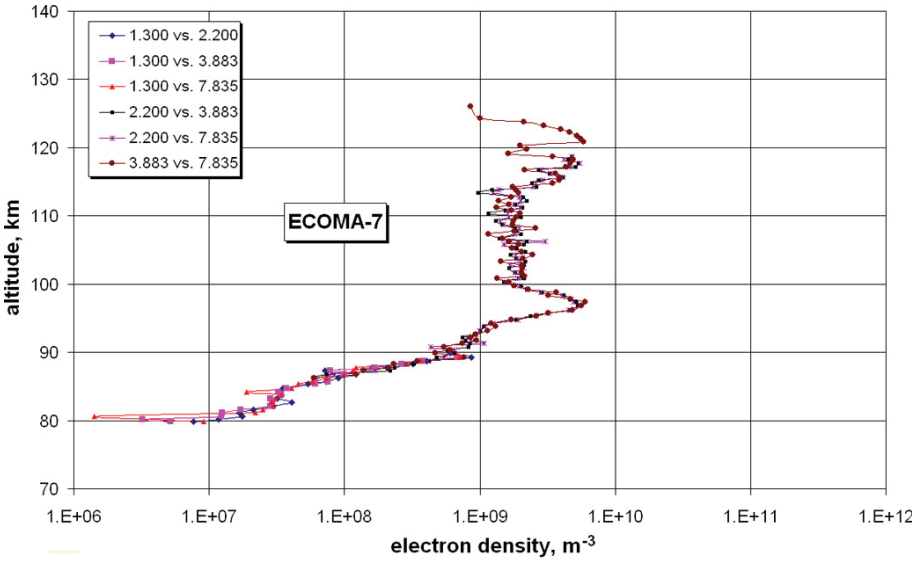

Fig. 2. Electron densities from the radio wave propagation experiment (flight ECOMA-7). In this flight all results are based on differential Faraday rotation, e.g. 2.200 vs. 3.883 etc.

whereof the outer one has the negative bias. This grid therefore collects ions, the current of which is monitored by a linear housekeeping channel. We process the data (currents) as for a plane Langmuir probe biased for ions. The grid biased at −3 V accelerates the ions with typical mass 32 amu to a velocity of about 4.3 km s^{-1}, i.e. larger that the rocket velocity. The ion density calculation ignores the rocket velocity of typically only 1 km s^{-1}, which we consider permissible in view of other uncertainties.

3 Results

3.1 ECOMA-7

The rocket ECOMA-7 was launched on 4 December 2010, at 04:21 UT. The solar zenith angle was 112.9°, the solar flux was 87.4 sfu and the number of sunspots on that day was 31 (for a summary of the flight conditions, see Table 1). Figure 2 shows the electron density results from the RWP (radio wave propagation) experiment due to the various sounding frequencies. Because of the extremely small electron density, the 3.883 MHz signal could be used all the way to apogee, and the highest frequency (7.835 MHz) only served as a spatial reference. The phase values (Faraday rotation) were not entered at equidistant increments of flight time, but rather in steps that were chosen to roughly correspond to 0.5 km of altitude. The profile RWP, used for comparisons with the various probes, is based on weighing the results of the various datasets (Faraday rotation, differential absorption, different frequencies, etc.) according to their respective sensitivity and reliability.

As mentioned above, only three of the four needles of the m-NLP provided data; however the relation of the currents of these three remaining needles still provides a check of the reliability of the data. The resulting electron density profile depicted in Fig. 3 shows much more detail than RWP, which is based on wave propagation only and appears to be too large by a factor of about 2.30 at the prominent peak at 97 km.

Applying Eq. (2) to the FEP data yields a profile 8.09 times larger at 97 km than RWP. The relative variations appear to be consistent with both the wave propagation results and the multi-needle probe (m-NLP). The FEP profile normalised at 97 km is up to a factor of 10 larger than the RWP profile below 85 km. This part of the FEP profile is much more akin to those of instruments measuring ions (see below).

The currents of the spherical positive ion probe (PIP) were converted to ion density assuming “reasonable” thermal velocities of the ions together with the known parameters such as the probe diameter, the grid transparency and the rocket velocity. The resulting ion density profile is too large by a factor of 3.09 at 97 km. Expectedly, below 86 km this factor becomes larger due to the presence of negative ions.

The current to the outer grid of the ECOMA instrument was considered housekeeping data and was only measured by a linear amplifier. As a result the threshold (first quantisation level) corresponds to a current which in this flight was only exceeded in consecutive telemetry samples at 86 km and above. The profile below that height down to 80 km in Fig. 3 is therefore not considered a reliable measurement. Between 86 and 95 km, the ion density deduced from the ECOMA grid is consistently somewhat larger than that from PIP; this may be due to discrimination of heavier ions/charged particles by PIP with its relatively low bias of only −2.5 V. Otherwise

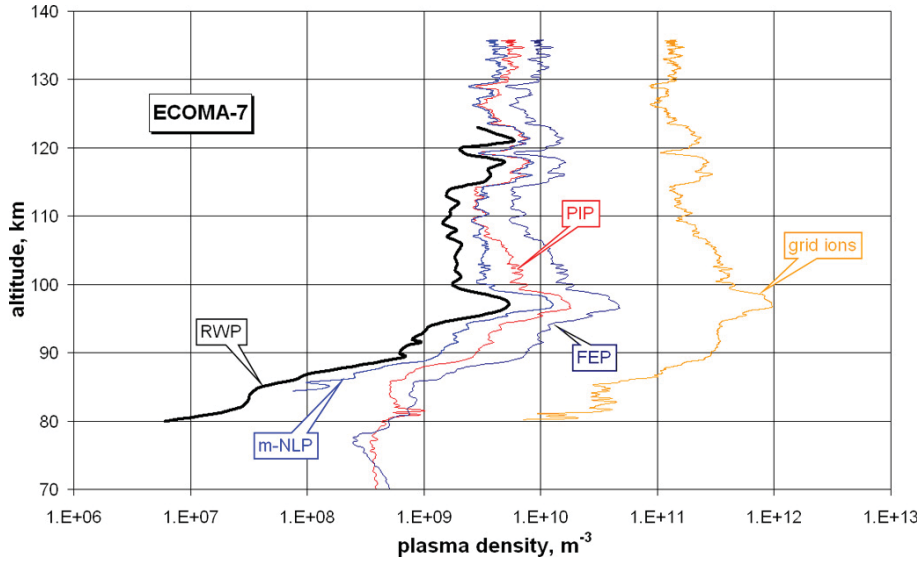

Fig. 3. Nominal (uncalibrated) plasma densities due to the various probes together with the absolute values RWP from the wave propagation instrument (flight ECOMA-7).

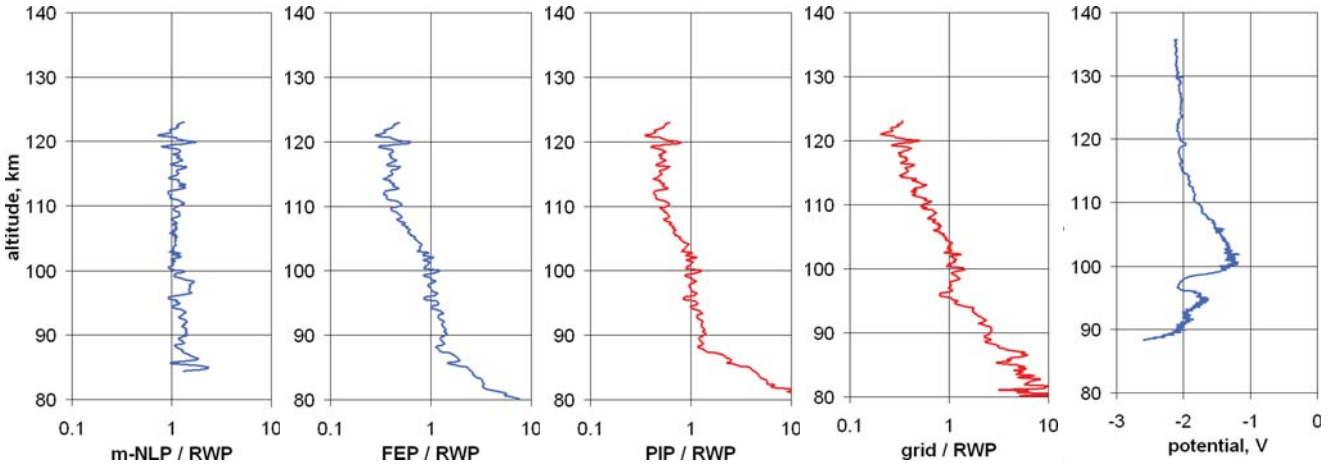

Fig. 4. Residual deviation from the RWP profile as a function of altitude of the various probes together with the measured payload potential (flight ECOMA-7).

these data provide the best height resolution since no spin-related variation is observed in the data; however, credible results only begin above 86 km and the nominal values are excessively larger by a factor of 170 (!).

Next, we shift all probe profiles to match the RWP data at 97 km and form the ratio between the probe plasma densities and the wave propagation data RWP. This normalisation altitude is chosen just above the height where negative ions (or negatively charged dust) may conceivably exist (cf. the accompanying paper by Friedrich et al., 2012). Figure 4 shows the residual variation of the deviations with altitude. Clearly, the multi-needle Langmuir probe data not only shows the smallest deviation, but also displays the least altitude variation of this factor.

At low altitudes (<85 km) the ion density is expected to exceed that of electrons due to the presence of negative ions. The fact that the (normalised) ECOMA shielding grid measures more ions than the dedicated gridded sphere (PIP) in the region of 86 to 95 km can tentatively be explained by the presence of heavy negative charges such as large water cluster ions, or indeed charged aerosols, which are not fully collected by the low bias of only −2.5 V on the inner collector of PIP (Pürstl, 2000), whereas a mass discrimination of the exposed grid is less pronounced.

3.2 ECOMA-8

ECOMA-8 was launched on 13 December 2010, at 03:24 UT. The solar zenith angle was 119.1°, the solar flux 87.7 sfu,

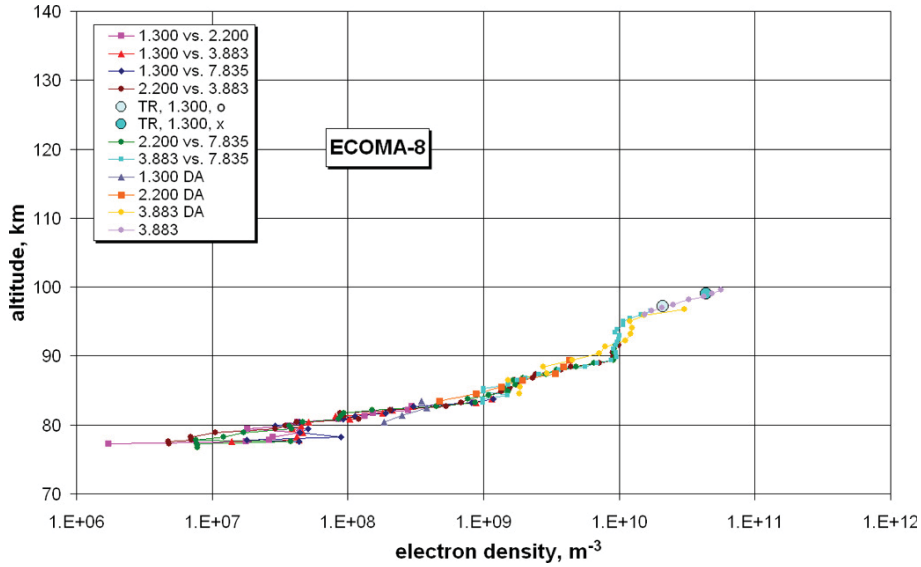

Fig. 5. Electron densities from various sources of the radio wave propagation experiment (flight ECOMA-8). When the rocket was at 100 km, the 7.835 MHz ground transmitter failed, and the three lower frequencies were all either absorbed or reflected (TR: total reflection [o and x modes]; DA: differential absorption).

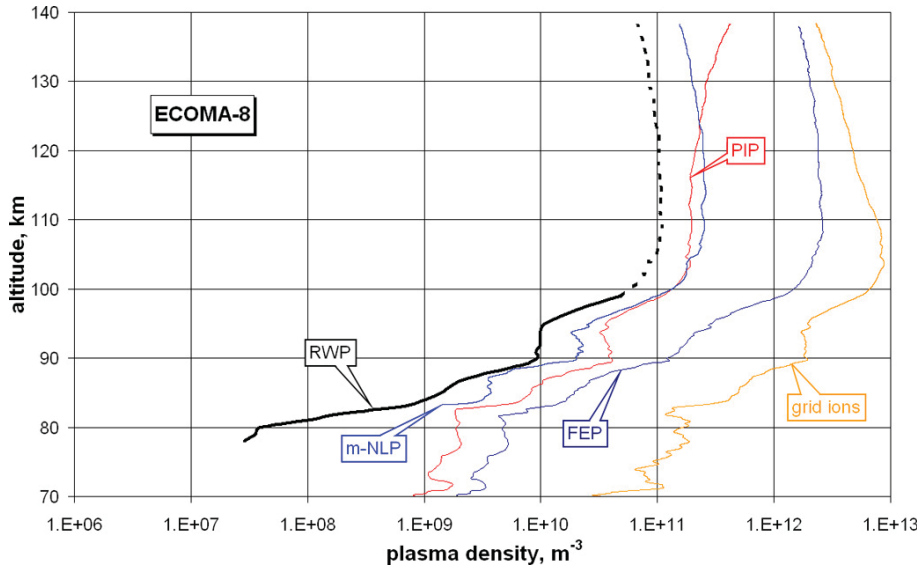

Fig. 6. As Fig. 3, but flight ECOMA-8. The dotted line is an extension of the RWP data primarily relying on the normalised data from the forward electron probe FEP and the multi-needle probe (m-NLP).

and there were 28 sunspots on that day. The ionosphere was more disturbed than either ECOMA-7 or -9. Unfortunately, the transmitter of the highest frequency (7.835 MHz) failed when the rocket was at 100 km and the lower frequencies could no longer be received above that height due to the large electron density. Otherwise, up to that height the data from the wave propagation instrument are very good (Fig. 5). Figure 6 shows the RWP together with the nominal (i.e. un-normalised) results of the various probes. The dashed line is based on the normalised profiles from FEP and the m-NLP; we again adjust all probe profiles at 97 km to the radio wave propagation results. FEP electron densities at lower altitudes (<83 km) are reminiscent of the ion densities due to PIP or the ECOMA grid. Whether the payload potential is responsible for that behaviour is doubtful, particularly since the ion-like behaviour of FEP is evident at an altitude where the payload potential is not excessively negative (Fig. 7). In contrast to the case of ECOMA-7, there is no identifiable difference between the (normalised) ion densities obtained from PIP or the ECOMA grid.

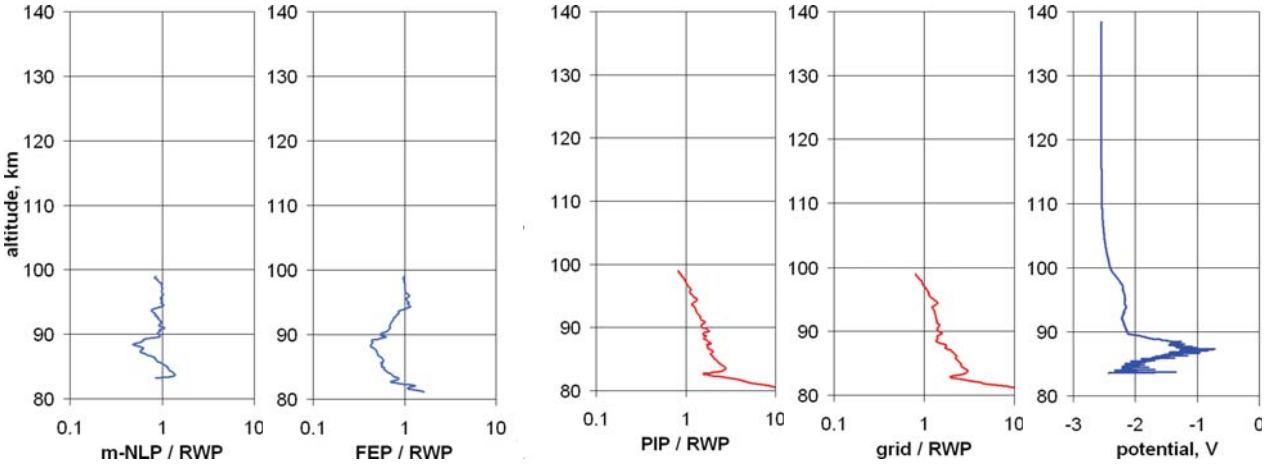

Fig. 7. As Fig. 4, but flight ECOMA-8.

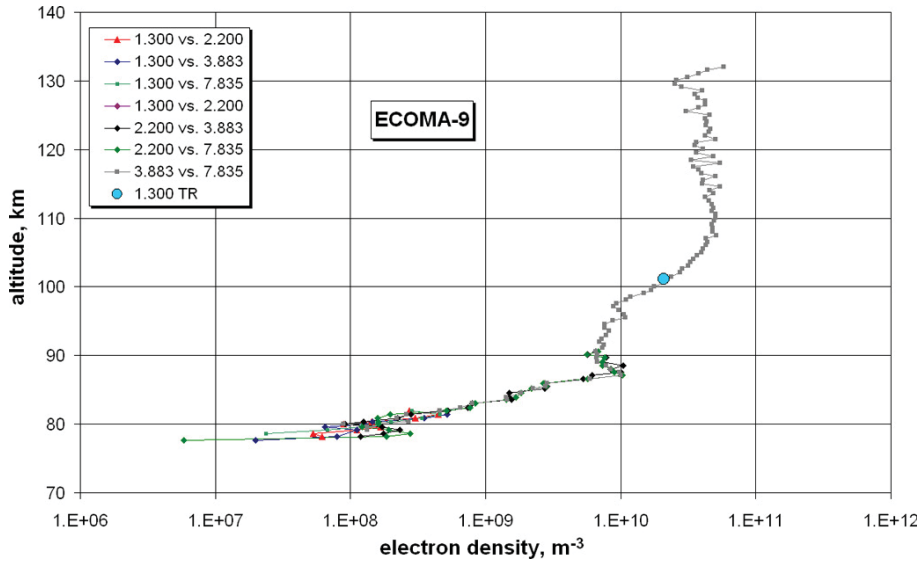

Fig. 8. As Fig. 2, but flight ECOMA-9.

3.3 ECOMA-9

ECOMA-9 was launched on 19 December 2010, at 02:36 UT. The solar zenith angle was 123.6°, the solar flux 80.9 sfu, and there were no sunspots on that day. The electron densities during this flight were small enough that the highest sounding frequency (7.835 MHz) was only needed as a spin reference, and we make use of differential Faraday rotation with different combinations of frequencies. In addition, the total reflection of the 1.300 MHz was very pronounced and thus yields an unambiguous electron density value (Fig. 8).

FEP again showed nominal values larger than RWP, namely by a factor of 22.2. More worrying is the shape of the FEP profile below 83 km since it too is almost identical to those of instruments measuring ions (PIP and ECOMA grid). Since the derived payload potential is always at least −2.5 V, proper operation as a saturated Langmuir probe is doubtful (Fig. 9).

The multi-needle probe results are closest to the combined wave propagation results (RWP) and also show the least height variation of the deviation (Fig. 10). Due to the plasma densities being somewhat larger than in the case of ECOMA-7, measurements using the grid current are credible down to 70 km.

4 Conclusions

Because radio wave propagation results (Faraday rotation, [differential] absorption) are neither influenced by aerodynamics nor by the payload potential, they represent the reference for the other instruments measuring electron densities. The height resolution is only moderate since it is tied

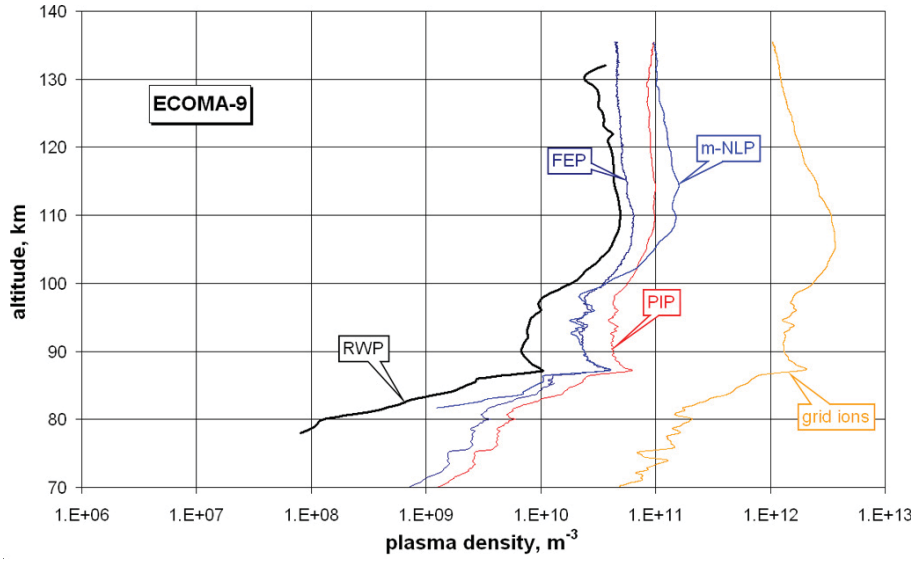

Fig. 9. As Fig. 3, but flight ECOMA-9.

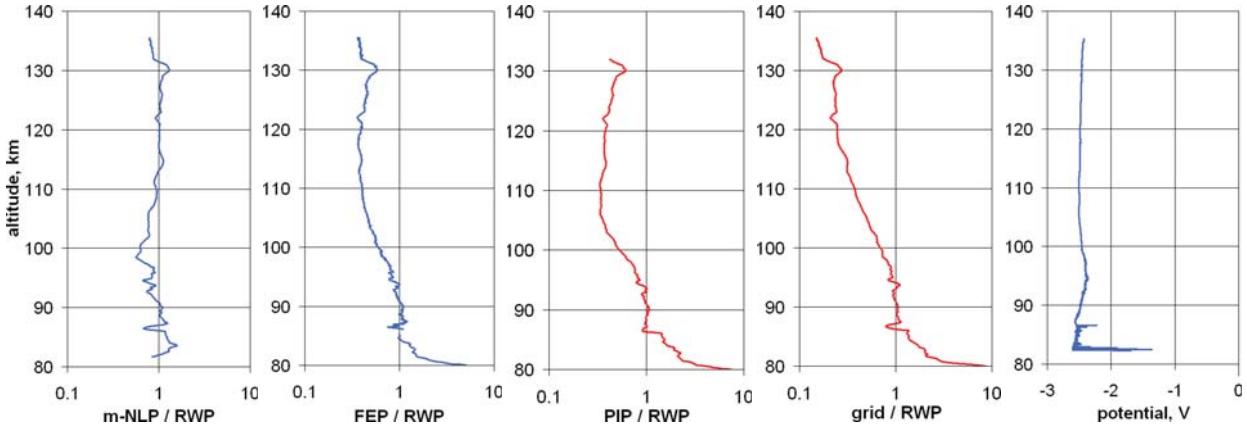

Fig. 10. As Fig. 4, but flight ECOMA-9.

to the rocket's spin rate, but owing to the narrow bandwidth of today's receivers (300 Hz) and the stable ionosphere conditions, the data quality – including absorption – is very good. The detection limit is primarily related to the collision frequency (i.e. proportional to pressure). In the case of ECOMA-7, usable measurements extend down to $10^7\,m^{-3}$ (at 80 km). In the other two flights the electron densities are larger at lower altitudes (i.e. at larger collision frequencies). At these larger collision frequencies, the threshold for the electron density measurements is consequently larger by about a factor of 2. This is in qualitative agreement with the simulated detections limits according to Jacobsen and Friedrich (1979).

The multi-needle Langmuir probe provides electron densities that are closest to the wave propagation values and only show a small residual height-dependence relative to RWP. Due to the probe arrangement, measurements only commenced after payload separation at about 83 km, and a test of the performance of this novel probe at even lower altitudes remains to be done. Apparently the method with different biases can indeed remove the influence of the payload potential, but it is still subject to aerodynamics, i.e. the location of the probes in relation to the shock cone; the aerodynamic impact is an issue in the present flights in the relatively dense mesosphere. The problem did not exist for the earlier flights from Spitsbergen and Poker Flat where the agreement at higher altitudes with ground-based, incoherent scatter data was close to unity. A simulation of the aerodynamics of a payload of a similar geometry and dimensions revealed that at the location of the m-NLP the needles are not outside the shock cone. In fact, this simulation suggests that the maxima are about a factor of two larger than the undisturbed ambient, whereas the minima in the spin period should correspond to only a small angle between payload axis and

Table 2. List of ECOMA flights with technical data of the various probes. In the last four columns, the deviation factors are given by which the nominal probe results have to be reduced for agreement with the respective wave propagation electron densities at 97 km on upleg. The values in brackets apply when using the *minima* in a spin period (see text).

Code	N_e @ cal.	FEP		ECOMA grid		m-NLP (1.1 cm^2 each needle)				FEP	ECOMA grid	m-NLP	PIP
	altitude 97 km m^{-3}	bias V	area cm^2	bias V	area cm^2	bias V	bias V	bias V	bias V	factor	factor	factor	factor
ECOMA-3	1.05×10^{10}	+2.5	8.3	−3.0	33.3					2.66	177		2.49
ECOMA-4	7.75×10^{10}	+2.5	13.2	−3.0	33.3					3.63	75.4		1.49
ECOMA-5	9.36×10^{9}	+2.5	13.2	−3.0	33.3					7.56	268		3.87
ECOMA-6	8.20×10^{10}	+2.5	13.2	−3.0	33.3					3.10	65.3		1.19
ECOMA-7	5.43×10^{9}	+2.5	1.5	−3.0	66.4	+2.50	+3.37	+4.29	+5.10	8.09	170	2.20 (1.37)	3.09
ECOMA-8	2.08×10^{10}	+2.5	1.5	−3.0	33.3	+2.50	+3.37	+4.29	+5.10	24.0	137	2.30 (0.93)	2.91
ECOMA-9	9.50×10^{9}	+2.5	1.5	−3.0	66.4	+2.50	+3.37	+4.29	+5.10	2.54	170	3.24 (0.92)	5.50

velocity vector, and result in values closer to the undisturbed ionosphere (Barjatya and Swenson, 2006). We use the minima in each spin period to test this hypothesis, which leads to profiles that are only factors 1.37, 0.93 and 0.92 from RWP results (ECOMA-7, -8, and -9, respectively). The conclusion thus is that the booms for the m-NLP probe were simply not long enough at that location at the rear of the payload, whereas had they been attached at the forward deck, the needles would have sampled the undisturbed ionosphere.

Strangely, the plane grid at the entrance of the ECOMA detector in some cases shows less altitude dependence of the deviation relative to RWP than the spherical gridded ion probe. The measured currents do not show any spin signatures because this grid is mounted exactly in the rocket axis; hence, the current provides a time resolution for the ion density, only limited by the telemetry sampling rate. Using an altitude-dependent normalisation, one can thus obtain the best height resolution of all the plasma instruments. The present measurements are restricted to larger densities because only a linear housekeeping channel was available for monitoring the current to the grid.

The profiles of both forward probes (FEP and PIP), after normalisation to RWP at 97 km, show a deficit above 100 km. Since it affects both species, it is not likely to be caused by a change in the payload potential, but must rather be related to some aerodynamic effect. Also, a decaying of the ionosphere during the flight can be ruled out since this decrease of the deviation is a feature observed in all three flights; notably, in flight ECOMA-9 the downleg data are actually larger by a factor of 2, hence the ionospheric densities *increased* during the measurement. Below about 85 km the fixed-bias, forward electron probes measured almost as much as the dedicated ion probes. The relatively large negative payload potential of 2 to 2.5 V may have caused this behaviour. Why the payloads ECOMA-7 to -9 should have charged more negative than the earlier ECOMA payloads is still unknown. According to simulations of these payloads (see the accompanying paper by Bekkeng et al., 2013), the main source of the negative charge is the positively biased grid of the CONE instrument at the rear of the payload. However, this instrument was part of all ECOMA payloads, including the flights where FEP definitively measured electrons (i.e. never more electrons than ions). The earlier ECOMA flights (all in daylight) had no instrument to measure the payload potential, but the "correct" performance of FEP and PIP suggests that there was no excessive negative potential, i.e. FEP measured a profile essentially simply shifted by a fairly constant factor relative to the RWP profile. The behaviour of FEP in flights 7 to 9, different from the earlier flights 3 to 6, cannot be explained by the absence of sunlight and, in consequence, absence of photoemission. Similar Langmuir-type probes were flown in full darkness (two each from Alcântara, Brazil, and from northern Scandinavia) and behaved expectedly, i.e. the measurements yielded more positive ions than electrons.

The behaviour of the probes described here differs significantly from that observed in four equatorial rocket flights (Friedrich et al., 1997). In 1994 two rockets each were launched from Alcântara, Brazil, near local noon and local midnight, respectively. The efficiency of both PIP and a hemispherical Langmuir probe was distinctly higher in darkness, and the cylindrical Langmuir probe (similar to FEP in the ECOMA flights) was only 10 % from the final electron densities. The payload potential was measured using a pair of spheres on relatively short booms; such a configuration is of course not as sophisticated as the m-NLP on ECOMA, but still the data suggest negative potentials never exceeding 1.3 V. Also the height dependence of the residual normalisation factors (cf. Figs. 4, 7 and 10) of the various probes showed much less variation with altitude than in the ECOMA flights.

The correlation between the payload potential structure and the various probe-derived plasma densities is not very obvious, but perhaps a little more apparent when the plasma densities are low. A perfect height-independent deviation close to unity cannot reasonably be expected since the wave propagation instrument relies on (a) only vertical structure of the ionosphere and (b) stable conditions during the passage of the rocket (ca. 1 min), whereas probes measure in

situ and are unaffected by conceivable temporal variations of the ionosphere underneath.

Table 2 lists the relevant features of the flights ECOMA-3 to -9, indicating the mean normalisation factors of the various probes when adjusted to RWP at 97 km. Despite the poor statistics of only seven flights, it is interesting that the normalisation factors of all probes – or probe proxies – (except for the m-NLP) come closer to unity for larger electron densities, both for electrons (FEP) and ions (PIP and grid), and no systematic difference between day and night-time data can be seen.

Acknowledgements. The Austrian participation in the ECOMA project was supported by Project 18560 of the Austrian Research Fund (FWF). The German part of the ECOMA project was funded by the German Space Agency (DLR) under grants 50 OE 0301 and 50 OE 0801, and the Norwegian part through the Norwegian Space Centre by grants 197629 and 191754.

Topical Editor C. Jacobi thanks E. Thrane and one anonymous referee for their help in evaluating this paper.

References

Barjatya, A. and Swenson, C. M.: Observations of Triboelectric Charging Effects on Langmuir-Type Probes in Dusty Plasma, J. Geophys. Res., 111, A10302, doi:10.1029/2006JA011806, 2006.

Bekkeng, T. A., Jacobsen, K. S., Bekkeng, J. K., Pedersen, A., Lindem, T., Lebreton, J.-P., and Moen, J. I.: Design of a Multi-Needle Langmuir Probe System, Meas. Sci. Technol., 21, doi:10.1088/0957-0233/21/8/085903, 2010.

Bekkeng, T. A., Barjatya, A., Hoppe, U.-P., Pedersen, A., Moen, J. I., Friedrich, M., and Rapp, M.: Payload charging events in the mesosphere and their impact on Langmuir type electric probes, Ann. Geophys., in press, 2013.

Folkestad, K.: Ionospheric Studies by in situ Measurements in Sounding Rockets, Internal NDRE Report 59 and PhD Thesis University of Oslo, 1970.

Friedrich, M. and Torkar, K. M.: Collision Frequencies in the High-Latitude D-Region, J. Atmos. terr. Phys., 45, 267–271, 1983.

Friedrich, M., Finsterbusch, R., Torkar, K. M., and Spöcker, P.: A Further Generalisation of the Sen and Wyller Magneto-Ionic Theory, Adv. Space Res., 11, 105–108, 1991.

Friedrich, M., Torkar, K. M., Goldberg, R. A., Mitchell, J. D., Croskey, C. L., and Lehmacher, G.: Comparison of Plasma Probes in the Lower Ionosphere, ESA SP-397, pp. 381–386, 1997.

Friedrich, M., Rapp, M., Blix, T., Hoppe, U.-P., Torkar, K., Robertson, S., Dickson, S., and Lynch, K.: Electron loss and meteoric dust in the mesosphere, Ann. Geophys., 30, 1495–1501, doi:10.5194/angeo-30-1495-2012, 2012.

Jacobsen, T. A. and Friedrich, M.: Electron Density Measurements in the Lower D-Region, J. Atmos. Terr. Phys., 41, 1195–1200, 1979.

Jacobsen, K. S., Pedersen, A., Moen, J. I., and Bekkeng, T. A.: A New Langmuir Probe Concept for Rapid Sampling of Space Plasma Electron Density, Meas. Sci. Technol., 21, doi:10.1088/0957-0233/21/8/085902, 2010.

Phelps, A. V. and Pack, J. L.: Electron Collision Frequencies in Nitrogen and in the Lower Ionosphere, Phys. Rev. Lett., 3, 340–342, 1959.

Pürstl, F.: MARIPROBE-D a 3D-Ion-Spectrometer for in-situ Investigation of Cold Ions in the Martian Ionosphere, Ph.D. Thesis, Technical University Graz, 2000.

Sen, H. K. and Wyller, A. A.: On the Generalization of the Appleton-Hartree Magnetoionic Formulas, J. Geophys. Res., 65, 3931–3950, 1960.

Smith, L. G.: Langmuir Probes in the Ionosphere, in: Small Rocket Techniques, North Holland, 1969.

Thrane, E. V. and Piggott, W. R.: The Collision Frequency in the D- and E-Regions of the Ionosphere, J. Atmos. Terr. Phys., 28, 721–737, 1966.